

Differential gene expression profiling of mouse skin after sulfur mustard exposure: Extended time response and inhibitor effect

Donald R. Gerecke^{a,*}, Minjun Chen^a, Sastry S. Isukapalli^a, Marion K. Gordon^a, Yoke-Chen Chang^a, Weida Tong^b, Ioannis P. Androulakis^c, Panos G. Georgopoulos^a

^a Environmental and Occupational Health Sciences Institute (EOHSI), a Joint Institute of UMDNJ-RW Johnson Medical School and Rutgers University, 170 Frelinghuysen Road, Piscataway, NJ 08854, USA

^b US FDA, National Center for Toxicological Research, Jefferson, AK, USA

^c Department of Biomedical Engineering, Rutgers, The State University of New Jersey, Piscataway, NJ, USA

ARTICLE INFO

Article history:

Received 7 July 2008

Revised 4 September 2008

Accepted 17 September 2008

Available online 7 October 2008

Keywords:

Vesicant

Sulfur mustard

Microarray

Alkylating agent

Skin

MMP inhibitor

MMP

Matrix metalloproteinase

ABSTRACT

Sulfur mustard (HD, SM), is a chemical warfare agent that within hours causes extensive blistering at the dermal–epidermal junction of skin. To better understand the progression of SM-induced blistering, gene expression profiling for mouse skin was performed after a single high dose of SM exposure. Punch biopsies of mouse ears were collected at both early and late time periods following SM exposure (previous studies only considered early time periods). The biopsies were examined for pathological disturbances and the samples further assayed for gene expression profiling using the Affymetrix microarray analysis system. Principal component analysis and hierarchical cluster analysis of the differently expressed genes, performed with ArrayTrack showed clear separation of the various groups. Pathway analysis employing the KEGG library and Ingenuity Pathway Analysis (IPA) indicated that cytokine–cytokine receptor interaction, cell adhesion molecules (CAMs), and hematopoietic cell lineage are common pathways affected at different time points. Gene ontology analysis identified the most significantly altered biological processes as the immune response, inflammatory response, and chemotaxis; these findings are consistent with other reported results for shorter time periods. Selected genes were chosen for RT-PCR verification and showed correlations in the general trends for the microarrays. Interleukin 1 beta was checked for biological analysis to confirm the presence of protein correlated to the corresponding microarray data. The impact of a matrix metalloproteinase inhibitor, MMP-2/MMP-9 inhibitor I, against SM exposure was assessed. These results can help in understanding the molecular mechanism of SM-induced blistering, as well as to test the efficacy of different inhibitors.

© 2008 Elsevier Inc. All rights reserved.

Introduction

Sulfur mustard [bis(2-chloroethyl)sulfide] (sulfur mustard, SM, HD) is a potent alkylating agent which penetrates the skin rapidly causing skin blistering within hours (Fig. 1A). The fluid filled blisters occur at the level of the dermal–epidermal junction (DEJ) which is also the identical pathological target for Junctional Epidermolysis Bullosa (JEB) (Monteiro-Riviere et al., 1999) JEB is a genetic skin blistering disease where the epidermis separates away from the dermis and compromises the skin integrity. Disruption of the dermal–epidermal junction in JEB appears to be further magnified through the actions of matrix metalloproteinases (MMPs), a family of proteases that both enhances the action of many activating factors during the inflammatory response, and contributes to tissue degradation (Yancey, 2005). Currently, there is no established pharmacological countermeasure

against SM-induced skin injury. Because the precise mechanisms responsible for SM-induced skin injury are unknown, treatment strategies and pharmacological countermeasures continue to be developed. Our previous work identified matrix metalloproteinase-9 (MMP-9) as a potential target of therapy for SM damage in that it quantitatively increases over time in response to sulfur mustard exposure (Shakarjian et al., 2006). Since this increase in MMP-9 correlates to increased tissue damage, it is hypothesized that a quantitative reduction of MMP-9 in skin would reduce the tissue damage normally observed after SM exposure. Studies have shown some success in the use of protease inhibitors both *in vitro* in cell culture (Cowan et al., 2000) and in an *in vivo* mouse model (Powers et al., 2000). It was tested whether or not topical skin treatment with MMP-2/MMP-9 inhibitor I [(2R)-2-[(4-Biphenyl)sulfonyl]amino]-3-phenylpropionic acid (Fig. 1B), was effective in reducing the secondary damage caused by MMP-9. Using microarray analysis, the major gene pathways that are activated in response to SM skin exposure were identified. The rationale for using microarray technology was that it may identify potential new target molecules or pathways that could

* Corresponding author. Fax: +1 732 445 0119.

E-mail address: gerecke@eohsi.rutgers.edu (D.R. Gerecke).

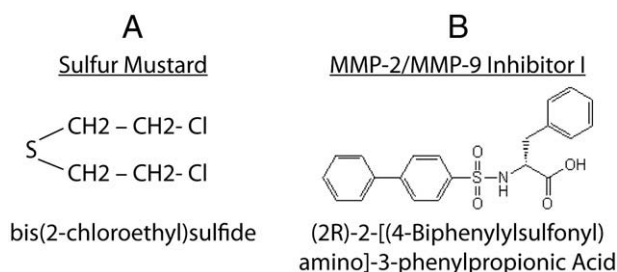


Fig. 1. Chemical structures of Sulfur Mustard and the MMP inhibitor.

be used for medical intervention against SM-induced injury. It also has the potential to identify biomarkers that could be used as quantitative tools for novel compound evaluation.

To date, there have only been a handful of microarray studies involving analysis of mouse skin treated with sulfur mustard (Rogers et al., 2004; Sabourin et al., 2004; Dillman et al., 2006). These studies only focused on gene changes at early time points within the first 24 h post exposure. The present study expanded the observed time-course to seven days in length. It also analyzed the impact of a specific MMP inhibitor to the SM-induced skin damage by assessing ear tissues from mice exposed to SM for histological damage (with and without topical pre-treatment with MMP-2/MMP-9 inhibitor I). Since microarray analysis data vary according to the method employed, analysis was performed using several different techniques in order to compare the gene variations with and without MMP-2/MMP-9 inhibitor I application and generate statistically significant data. A majority of the techniques employed in this study to analyze gene expression microarray data are supported by the USFDA's ArrayTrack system (Tong et al., 2003; 2004). In the present study, the multiple analysis methods supported by ArrayTrack were used, both within ArrayTrack and through links to other analysis platforms.

Methods

Experimental design. A schematic depiction of the experiments and subsequent analysis is shown in Fig. 2. The mice were divided into three groups (each group is represented by three post-exposure time-points). The three groups included: 1) untreated, control group; 2) mice treated with sulfur mustard; 3) mice treated with sulfur mustard after pre-treatment with the inhibitor. The microarray gene expression data were then analyzed to identify the genes that have been significantly expressed using several different statistical and pathway analysis techniques. Details of the experiments and the analysis methods follow.

SM exposure. Animals were exposed to SM as reported in Shakarjian et al. (2006). Briefly, for the mouse ear exposures, male CD1 mice [Charles River Laboratories, Portage, MI; $N=20$ per treatment] anesthetized with ketamine and xylazine were exposed to 5 μ l of 97.5 mM SM (0.08 mg) in CH_2Cl_2 (methylene chloride) through application to the inner medial surface of the right ear]. The left ear served as a control and received only the vehicle CH_2Cl_2 . There were additional controls in the study that included untreated ear punches, ethanol alone (the carrier for the MMP 2/MMP 9 inhibitor I), inhibitor in ethanol, and inhibitor in ethanol followed by CH_2Cl_2 alone. A statistician analyzed all the study control results and concluded there was no significant difference in the microarray results for any of the controls (data not shown). At 24, 72, and 168 h post-exposure, animals were euthanized and dermal punch specimens (8 mm in diameter) were taken from the center of both the SM-exposed and control ears. The punch biopsies were collected for an early time period (24 h post-exposure) and late time periods (72 h and 168 h post-exposure). The ear punches were either snap-frozen in liquid nitrogen and stored at -70°C for microarray analysis or fixed in neutral-buffered formalin for 24 h at room temperature for histopathology analysis.

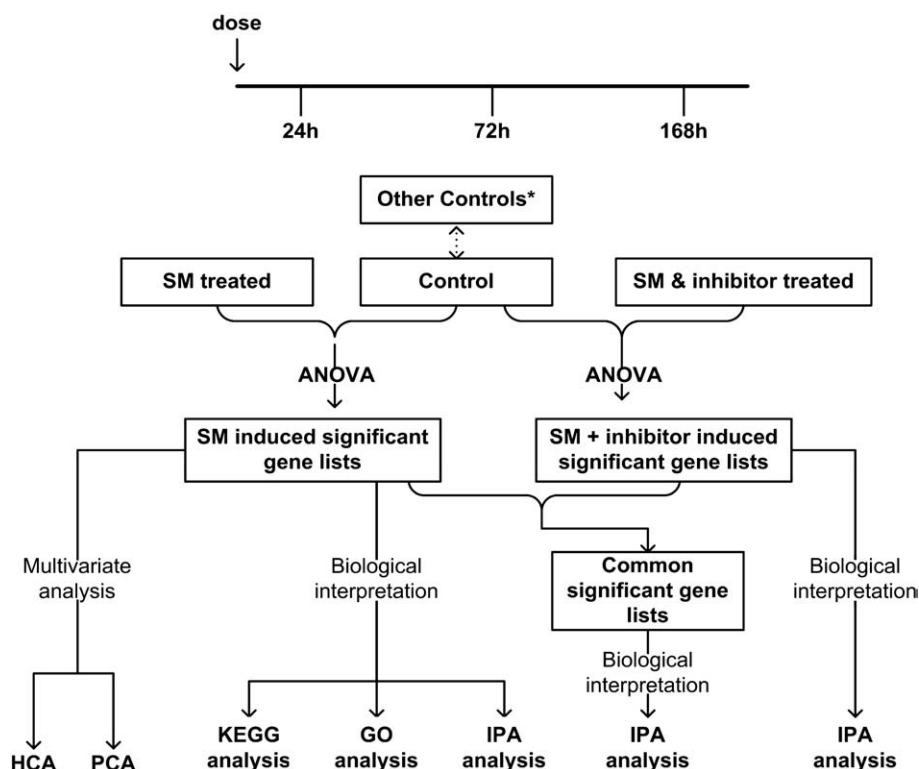


Fig. 2. Schematic depiction of the microarray experimental design and subsequent analyses. *Other controls are described in Methods section (a comparison of all the various control groups showed no significant differences between the groups).

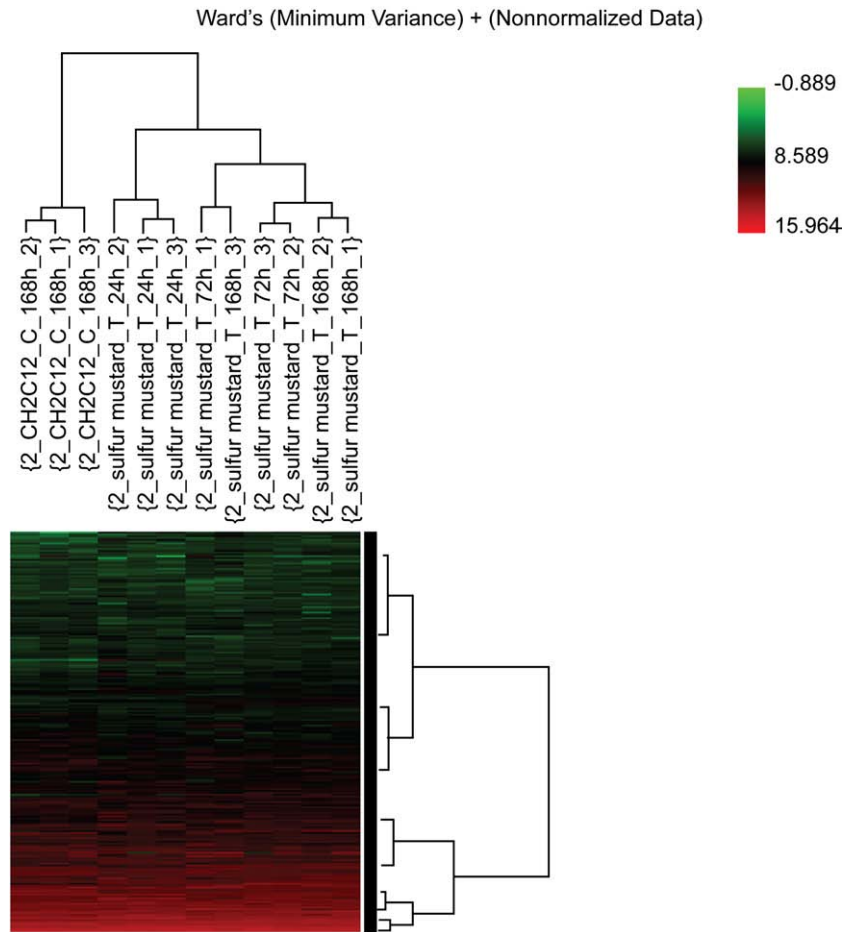


Fig. 3. Hierarchical cluster analysis (HCA) based on 24,681 genes whose mean channel intensities were greater than 100 in the arrays. The control group separates from the SM-treated group, with an increasing distance with the time after dosing. This indicates an increasing number of genes are activated following SM-induced cutaneous injury.

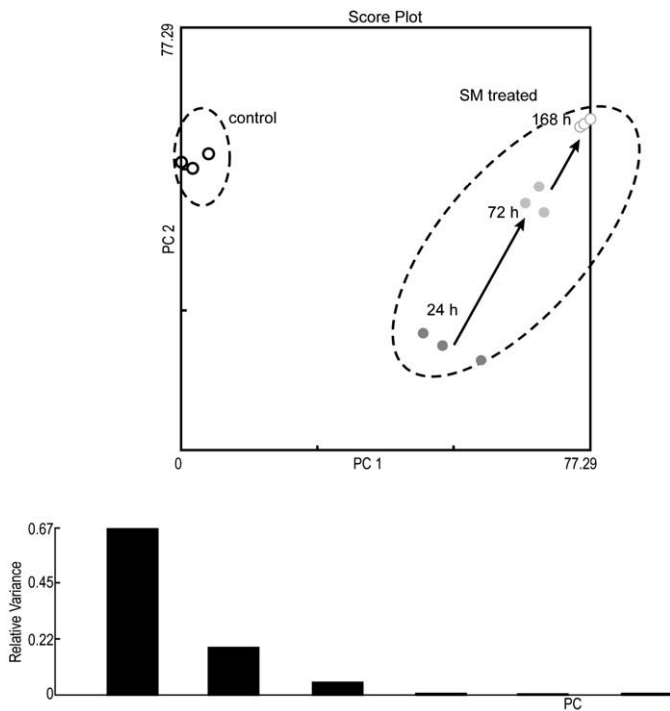


Fig. 4. Principle component analysis based on the 24,681 genes with mean channel intensities greater than 100 as measured across different time points after treatment. The control group clearly separates from the treated group, and a monotonous time-course trajectory of 24 h, 72 h, and 168 h was observed.

Microarray experiments. Between 5 and 20 ng of total RNA prepared from each tissue biopsy was used to generate a high fidelity cDNA for array hybridization. The cDNA were analyzed by electrophoresis using

Table 1
Pathways obtained from KEGG analysis at 24 h, 72 h and 168 h

Pathway name	Fisher <i>P</i> value
24 h	
Cytokine–cytokine receptor interaction	0.00002
Inositol phosphate metabolism	0.00064
Phosphatidylinositol signaling system	0.00651
Synthesis and degradation of ketone bodies	0.03842
Jak-STAT signaling pathway	0.03924
Hematopoietic cell lineage	0.04550
72 h	
Cytokine–cytokine receptor interaction	0.00000
Hedgehog signaling pathway	0.00190
Cell communication	0.00822
Jak-STAT signaling pathway	0.02221
168 h	
Cytokine–cytokine receptor interaction	0.00001
Cell adhesion molecules (CAMs)	0.00017
Hematopoietic cell lineage	0.00500
Neuroactive ligand–receptor interaction	0.00776
Glycosphingolipid biosynthesis – neo-lactoseries	0.02207
Jak-STAT signaling pathway	0.04376
Complement and coagulation cascades	0.04682

Here Fisher *P* value indicates the pathway's significance compared with chance sampling alone. Cytokine–cytokine receptor interaction, cell adhesion molecules (CAMs), hematopoietic cell lineage are common pathways at different time points.

Table 2

The top biological functions generated by IPA for the significant genes list of 24 h, 72 h, and 168 h

Biological function	-log (p-value)/genes		
	24 h	72 h	168 h
Cell death	17.5 (511)	17.3 (528)	17.3 (580)
Cancer	12.6 (566)	17.2 (623)	14.2 (687)
Inflammatory disease	11.5 (226)	17.8 (271)	18.4 (295)
Immunological disease	10.3 (228)	17.1 (260)	18.5 (287)
Cell movement	9.5 (311)	12.5 (323)	22.6 (401)

P-value represents the statistical significance of the specific biological function, and -log(p-value) increases with the statistical significance (-log(p-value)=1.30 when p-value=0.05). The number under the dash represents that the number of genes in a gene list was involved in a biological function. Results in this table shows that inflammation plays an important role in the etiology of SM-induced cutaneous injury. The total number of genes affected are in parentheses.

Table 3

Genes involved in inflammatory response induced by sulfur mustard at 24, 72 and 168 h post-exposure

Gene name	Gene description	Fold change (SM)		
		24 h	72 h	168 h
Bax	BCL2-associated X protein	3.38 [†]	2.56 [†]	2.23 [†]
Bid	BH3 interacting domain death agonist	1.97 [†]	2.54*	2.08*
Bsg	Basigin (Ok blood group)	2.00*	1.56	1.05
C5ar1	Complement component 5a receptor 1	2.62*	3.53*	6.09*
Ccl2	Chemokine (C-C motif) ligand 2	10.71*	9.35 [†]	4.17*
Ccl6	Chemokine (C-C motif) ligand 6	4.09 [†]	5.19 [†]	4.50*
Ccr1	Chemokine (C-C motif) receptor 1	12.20 [†]	15.04 [†]	20.58 [†]
Ccr2	Chemokine (C-C motif) receptor 2	2.36*	3.31 [†]	3.07 [†]
Ccr5	Chemokine (C-C motif) receptor 5	6.93 [†]	8.57 [†]	10.33 [†]
Cd14	CD14 molecule	5.97 [†]	9.34 [†]	13.86 [†]
Cd44	CD44 molecule (Indian blood group)	2.23 [†]	2.27 [†]	2.10 [†]
Cd47	CD47 molecule	1.10	1.21	1.78*
Cebpd	CCAAT/enhancer binding protein (C/EBP), delta	1.62*	2.25 [†]	1.97*
Cfb	Complement factor B	1.70*	2.39 [†]	2.31*
Cxcl2	Chemokine (C-X-C motif) ligand 2	270.81 [†]	286.62 [†]	497.50 [†]
Dmd	Dystrophin (muscular dystrophy, Duchenne and Becker types)	-2.07 [†]	-1.26*	1.89
Dsg3	Desmoglein 3 (pemphigus vulgaris antigen)	2.61*	2.46*	1.62
Egr1	Early growth response 1	2.39 [†]	1.52	1.28
F3	Coagulation factor III (thromboplastin, tissue factor)	-1.89 [†]	-1.75*	-1.96 [†]
Fas	Fas (TNF receptor superfamily, member 6)	2.88 [†]	2.10*	1.89 [†]
Fcgr2b	Fc fragment of IgG, low affinity IIb, receptor (CD32)	4.10 [†]	5.19 [†]	8.15 [†]
Hexb	Hexosaminidase B (beta polypeptide)	-1.55*	-1.09	-1.15
Icam1	Intercellular adhesion molecule 1 (CD54), human rhinovirus receptor	3.86 [†]	2.78 [†]	3.81 [†]
Il18	Interleukin 18	-2.56*	-1.08	-1.15
Il1b	Interleukin 1, beta	35.29*	34.18 [†]	51.94 [†]
Il1rl1	Interleukin 1 receptor-like 1	3.79*	8.37*	18.77*
Il1rn	Interleukin 1 receptor antagonist	1.84*	1.18	1.72
Il6	Interleukin 6	26.54 [†]	12.51 [†]	16.61 [†]
Insr	Insulin receptor	1.51	1.76	2.84*
Itgb1	Integrin, beta 1	2.78*	2.30	5.60
Itgb2	Integrin, beta 2	2.42*	3.56 [†]	3.12 [†]
Lbp	Lipopolysaccharide binding protein	1.97*	1.58*	1.26
Lgals1	Lectin, galactoside-binding, soluble, 1	1.50 [†]	2.31 [†]	1.73 [†]
Map2k1	mitogen-activated protein kinase kinase 1	1.69*	2.27*	2.02 [†]
Map3k7	Mitogen-activated protein kinase kinase kinase 7	1.66 [†]	1.38 [†]	1.74*
Mif	Macrophage migration inhibitory factor	1.36*	1.19	1.82
Mmp9	Matrix metalloproteinase 9 (gelatinase B, 92 kDa gelatinase, 92 kDa type IV collagenase)	2.40*	3.93*	8.26 [†]
Myd88	Myeloid differentiation primary response gene (88)	1.56*	1.46	1.17
Nfe2l2	Nuclear factor (erythroid-derived 2)-like 2	1.33*	1.36*	1.35*
Nfkbia	Nuclear factor of kappa light polypeptide gene enhancer in B-cells inhibitor, alpha	1.66*	1.43	1.62*
Osm	Oncostatin M	4.47*	5.00*	8.46 [†]
Ptgs2	Prostaglandin-endoperoxide synthase 2	23.88 [†]	27.62 [†]	34.35 [†]

* p<0.05.

† p<0.01.

Table 4

Genes involved in p53 signaling pathway induced by sulfur mustard at 24, 72 and 168 h post-exposure

Gene name	Gene description	Fold change (SM)		
		24 h	72 h	168 h
Akt2	v-akt murine thymoma viral oncogene homolog 2	1.78 [†]	1.46*	1.41 [†]
Bax	BCL2-associated X protein	3.38 [†]	2.56 [†]	2.23 [†]
Ccnd1	Cyclin D1	1.87 [†]	1.67*	1.67 [†]
Ccng1	Cyclin G1	5.89 [†]	3.30*	2.73*
Chek2	CHK2 checkpoint homolog (S. pombe)	-1.04	2.10 [†]	1.79*
E2f1	E2F transcription factor 1	1.49	1.54	1.79*
Mdm2	Mdm2, transformed 3 T3 cell double minute 2, p53 binding protein	3.41 [†]	1.87 [†]	1.69*
Pik3c2g	Phosphoinositide-3-kinase, class 2, gamma polypeptide	-2.56 [†]	-2.13*	-2.44 [†]
Pik3cd	Phosphoinositide-3-kinase, catalytic, delta polypeptide	1.13	1.79	2.35*
Pik3cg	Phosphoinositide-3-kinase, catalytic, gamma polypeptide	1.29 [†]	2.35*	3.12 [†]
Pik3r5	Phosphoinositide-3-kinase, regulatory subunit 5, p101	2.01*	3.36*	4.14 [†]
Pmaip1	Phorbol-12-myristate-13-acetate-induced protein 1	6.84 [†]	3.93*	3.28*
Serpib5	Serpin peptidase inhibitor, clade B (ovalbumin), member 5	-1.25	-1.39*	-2.06*
Serpine2	Serpin peptidase inhibitor, clade E (nexin, plasminogen activator inhibitor type 1), member 2	1.95*	2.35*	3.99*
Trp53bp2	Tumor protein p53 binding protein2	-1.34*	-1.61*	-1.50
Trp53inp1	Tumor protein p53 inducible nuclear protein 1	2.75 [†]	1.45 [†]	1.36

* p<0.05.

† p<0.01.

Table 5

Genes involved in NF-κB signaling pathway induced by sulfur mustard at 24, 72 and 168 h post-exposure

Gene name	Gene description	Fold change (SM)		
		24 h	72 h	168 h
Akt2	v-akt murine thymoma viral oncogene homolog 2	1.78 [†]	1.46*	1.41 [†]
Ep300	E1A binding protein p300	-1.72*	-2.13*	-2.13*
Ghr	Growth hormone receptor	-1.66*	-1.52*	-1.18
Ikbkg	v-Ha-ras Harvey rat sarcoma viral oncogene homolog	1.59*	1.80 [†]	1.48*
Il1b	Interleukin 1, beta	35.29 [†]	34.18 [†]	51.94 [†]
Il1rn	Interleukin 1 receptor antagonist	1.84 [†]	1.18	1.72 [†]
Irak3	Interleukin-1 receptor-associated kinase 3	2.78*	1.98	1.77*
Map3k7	Mitogen-activated protein kinase 8	1.66 [†]	1.3 [†]	1.74*
Nfkbia	Nuclear factor of kappa light polypeptide gene enhancer in B-cells inhibitor, alpha	1.66*	1.43	1.62*
Nfkbie	Nuclear factor of kappa light polypeptide gene enhancer in B-cells inhibitor, epsilon	1.66	1.99	3.97*
Ngf	Nerve growth factor, beta polypeptide	13.52 [†]	11.37 [†]	6.15*
Pik3c2g	Phosphoinositide-3-kinase, class 2, gamma polypeptide	-2.56 [†]	-2.13*	-2.44 [†]
Pik3cd	Phosphoinositide-3-kinase, catalytic, delta polypeptide	1.13	1.79	2.35*
Pik3cg	Phosphoinositide-3-kinase, catalytic, gamma polypeptide	1.29*	2.35*	3.12 [†]
Pik3r1	Phosphoinositide-3-kinase, regulatory subunit 1 (p85 alpha)	1.03	-1.28*	-1.39*
Pik3r5	Phosphoinositide-3-kinase, regulatory subunit 5, p101	2.01*	3.36*	4.14 [†]
Rras2	Related RAS viral (r-ras) oncogene homolog 2	1.94*	1.98*	1.79 [†]
Tgfa	Transforming growth factor, alpha	1.57	2.36 [†]	2.24*
Tirap	Toll-interleukin 1 receptor (TIR) domain containing adaptor protein	1.73*	1.60*	1.54*
Tlr1	Toll-like receptor 1	3.13 [†]	6.83 [†]	5.76 [†]
Tlr2	Toll-like receptor 2	2.25	3.34*	3.75*
Tlr3	Toll-like receptor 3	1.05	1.56 [†]	2.22 [†]
Tlr4	Toll-like receptor 4	1.64	1.85 [†]	1.93*
Tnfaip3	Tumor necrosis factor, alpha-induced protein 3	3.12 [†]	1.23	2.95 [†]
Traf3	TNF receptor-associated factor 3	1.65*	1.72	2.18*

* p<0.05.

† p<0.01.

Table 6

Genes involved in oxidative stress pathway induced by sulfur mustard at 24, 72 and 168 h post-exposure

Gene name	Gene description	Fold change (SM)		
		24 h	72 h	168 h
Fos	v-fos FBJ murine osteosarcoma viral oncogene homolog	4.56*	2.70†	2.49*
Gpx1	Glutathione peroxidase 1	1.36	1.69	1.69*
Gss	Glutathione synthetase	1.48*	1.51*	1.40*
Gsta2	Glutathione S-transferase A5	-2.70	-1.92	-3.70*
Gstm2	Glutathione S-transferase M1	-1.52	-1.15	-1.59*
Gstm1	Glutathione S-transferase M5	-1.60	-1.77†	-2.00*
Gstm5	Glutathione S-transferase M3 (brain)	-1.33	-1.12	-1.82†
Icam1	Intercellular adhesion molecule 1 (CD54), human rhinovirus receptor	3.86†	2.78†	3.81†
Il6	Interleukin 6(interferon, beta 2)	26.54†	12.51†	16.61†
Mgst1	Microsomal glutathione S-transferase 1	1.24	1.36*	2.83*
Mpo	Myeloperoxidase	-1.18	-2.63*	-9.09*
Nfe2l2	Nuclear factor (erythroid-derived 2)-like 2	1.33†	1.36†	1.35†
Prdx3	Peroxisiredoxin 3	1.47	1.66†	1.60†
S100a9	S100 calcium binding protein A9	60.60†	71.55†	52.98†
Sod2	Superoxide dismutase 2, mitochondrial	1.46†	1.15	1.43*
Stat3	Signal transducer and activator of transcription 3	2.04*	1.67*	1.85*
Vcam1	Vascular cell adhesion molecule 1	1.56	1.18	3.05*

* $p < 0.05$.† $p < 0.01$.

the Agilent Bioanalyzer 2100 to assess the appropriate size distribution prior to microarray hybridization. 2.5 µg of amplified labeled cDNA was used in the hybridization cocktail for GeneChip analysis. Three technical replicates and three biological replicates were used in this study. All samples were subjected to gene expression analysis via the Affymetrix mouse 430_2.0 Plus high-density oligonucleotide array, which currently queries 46,000 mouse probe sets. Hybridization, staining and washing of all arrays were performed in the Affymetrix fluidics module as per the manufacturer's protocol. The detection and quantitation of target hybridization was performed with a GeneArray Scanner 3000 set to scan each array twice at a factory set PMT level and resolution. All arrays referred to in this study

Table 7

Genes involved in p38 MAPK pathway induced by sulfur mustard at 24, 72 and 168 h post-exposure

Gene name	Gene description	Fold change (SM)		
		24 h	72 h	168 h
Creb1	cAMP responsive element binding protein 1	2.92*	9.38*	7.89*
Ddit3	DNA-damage-inducible transcript 3	1.62*	1.23	1.14
Eef2k	Eukaryotic elongation factor-2 kinase	-1.58†	-1.80*	-1.60†
Fas	Fas (TNF receptor superfamily, member 6)	2.88†	2.10*	1.89†
H3f3a	H3 histone, family 3A	1.81*	1.05	1.17
H3f3b	H3 histone, family 3B (H3.3B)	2.10*	-1.13	-1.18
Il18	Interleukin 18 (interferon-gamma-inducing factor)	-2.56*	-1.08	-1.15
Il1b	Interleukin 1, beta	35.29†	34.18†	51.94†
Il1rn	Interleukin 1 receptor antagonist	1.84†	1.18	1.72
Irak3	Interleukin-1 receptor-associated kinase 3	2.78*	1.98	1.77
Map3k7	Mitogen-activated protein kinase kinase kinase 7	1.66†	1.38*	1.74*
Mapk13	Mitogen-activated protein kinase 13	-1.56*	1.16	-1.30
Mef2a	Myocyte enhancer factor 2A	-1.00	1.41*	1.74*
Pla2g4b	Phospholipase A2, group IVB (cytosolic)	1.48*	1.69*	1.40
Rps6ka4	Ribosomal protein S6 kinase, 90 kDa, polypeptide 4	1.87†	1.92†	1.60†
Rps6ka5	Ribosomal protein S6 kinase, polypeptide 5	-1.61†	-1.13	1.41
Stat1	Signal transducer and activator of transcription 1	1.49*	1.56*	1.73†
Tgfb2	Transforming growth factor, beta 2	-1.70*	-1.89*	-1.68*
Tgfb3	Transforming growth factor, beta 3	-4.17†	-1.67	-1.54
Tradd	TNFRSF1A-associated via death domain	1.54†	1.33	1.22

* $p < 0.05$.† $p < 0.01$.**Table 8**

Genes involved in pro-apoptosis induced by sulfur mustard at 24, 72 and 168 h post-exposure

Gene name	Gene description	Fold change (SM)		
		24 h	72 h	168 h
Apaf1	Apoptotic peptidase activating factor 1	2.66*	2.17†	1.98
Bax	BCL2-associated X protein	3.38†	2.56†	2.23†
Bcl2l11	BCL2-like 11 (apoptosis facilitator)	2.41†	1.96	2.44*
Bid	BH3 interacting domain death agonist	1.97†	2.54*	2.08*
Bmf	Bcl2 modifying factor	1.30*	1.56	1.48
Fas	Fas (TNF receptor superfamily, member 6)	2.88†	2.10*	1.89†
Tnfrsf10b	Tumor necrosis factor receptor superfamily, member 10a	4.49*	2.83	2.05
Tradd	TNFRSF1A-associated via death domain	1.54†	1.33	1.22
Traf3	TNF receptor-associated factor 3	1.65*	1.72	2.18*

* $p < 0.05$.† $p < 0.01$.

were assessed for "array performance" prior to data analysis via statistical analysis of control transcripts that were spiked into the samples themselves and the hybridization cocktail.

Data analysis methods. The USFDA's ArrayTrack system (Tong et al., 2003; 2004) has been used with different analysis approaches for studying the microarray data from the experiments. ArrayTrack is an open platform and contains three integrated components: (a) MicroarrayDB, which stores essential data associated with a microarray experiment, including information on slide samples, treatment, and experimental results; (b) TOOL, which provides analysis capabilities for data visualization, normalization, significance analysis, clustering, and classification; and (c) LIB, which contains information from public and proprietary repositories (e.g., for gene annotation, protein function, and pathways). ArrayTrack is being enhanced to result in a new system, termed ebTrack, through additional analysis modules for gene expression data as well as through incorporation or linkages to modules for analysis of proteomic and metabolomic datasets that include tandem mass spectra. Furthermore, interfaces to environmental health risk analysis tools, as well as an open source database backend are planned in order to make it even more widely usable.

Gene expression data were first normalized using the Microarray Suite, version 5.0 (MAS5; Affymetrix), with an auto-scale intensity of 500. The normalized data were converted into log₂ intensity and only

Table 9

Genes involved in the apoptosis signaling pathway induced by sulfur mustard at 24, 72 and 168 h post-exposure

Gene name	Gene description	Fold change (SM)		
		24 h	72 h	168 h
Akt2	v-akt murine thymoma viral oncogene homolog 2	1.78†	1.46*	1.41†
Bax	BCL2-associated X protein	3.38†	2.56†	2.23†
Bid	BH3 interacting domain death agonist	1.97†	2.54*	2.08*
Capn3	Calpain 3, (p94)	1.47	1.61	2.16†
Capn5	Calpain 5	-2.20	-1.49	-2.44*
Casp8	Caspase 8, apoptosis-related cysteine peptidase	1.31	1.53*	1.72†
Fas	Fas (TNF receptor superfamily, member 6)	2.88†	2.10*	1.89†
Ikkg	Inhibitor of kappa light polypeptide gene enhancer in B-cells, kinase gamma	1.59*	1.80†	1.48*
Map2k1	Mitogen-activated protein kinase kinase 1	1.69*	2.27*	2.02†
Nfkbia	Nuclear factor of kappa light polypeptide gene enhancer in B-cells inhibitor, alpha	1.66*	1.43	1.62*
Nfkbie	Nuclear factor of kappa light polypeptide gene enhancer in B-cells inhibitor, epsilon	1.66	1.99	3.97*
Pak3	p21 (CDKN1A)-activated kinase 3	-1.69	-1.70†	-2.19†
Pkn1	Protein kinase N1	1.61	1.35	2.48*
Rras2	Related RAS viral (r-ras) oncogene homolog 2	1.94*	1.98*	1.79†
Ttk	TTK protein kinase	-1.24	1.04	-2.13*

* $p < 0.05$.† $p < 0.01$.

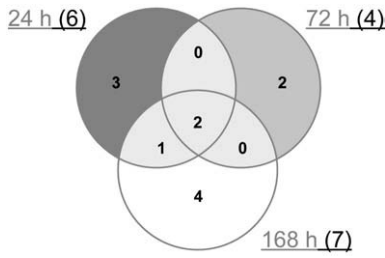


Fig. 5. Number of pathways obtained through KEGG analysis for those genes whose expression was significantly altered by sulfur mustard. At least 2 pathways were common for different time points.

those genes which were expressed with mean channel intensities greater than 100 were selected for further analysis. This represents about 24,681 genes out of a total of about 45,000. Principal Component Analysis (PCA) and Hierarchical Cluster Analysis (HCA) were then applied on the selected data using the centered method within ArrayTrack. Subsequently, significant genes were selected using cutoffs of $p < 0.05$ and fold change > 1.5 (and retaining the constraint that the mean intensity is greater than 100). The identification of differentially expressed genes was based on Welch t -test.

The initial genomic analysis used the methodology of the Gene Ontology (GO) Consortium. This initial analysis provided some

biological information and was followed by a KEGG pathway analysis (Kanehisa et al., 2004). Subsequently, Ingenuity Pathway Analysis (IPA) (Ingenuity Systems, 2008) was performed to gather even more information on individual gene changes and an attempt was made to link them to biological functions in the model system. Significantly expressed genes at 24 h, 72 h, and 168 h post-dosing were uploaded into IPA. When one gene corresponded to several spots in arrays, the average intensity was used as its gene expression response. LocusID of each gene was mapped to its corresponding gene object in the IPA Knowledge Base. These genes were then used as the starting point for calculating biological functions, and assigning them to different pathways and networks.

Real-time polymerase chain reaction. RT-PCR was performed as previously described (Shakarjian et al., 2006).

Cytokine enzyme quantitation. The interleukin 1 beta enzyme was quantitated using the Millipore Mouse Cytokine Lincplex system.

Results

The gene expression data were analyzed through different analysis techniques, including PCA, HCA, Gene GO analysis, KEGG pathway analysis, and IPA analysis. All the methods were consistent and

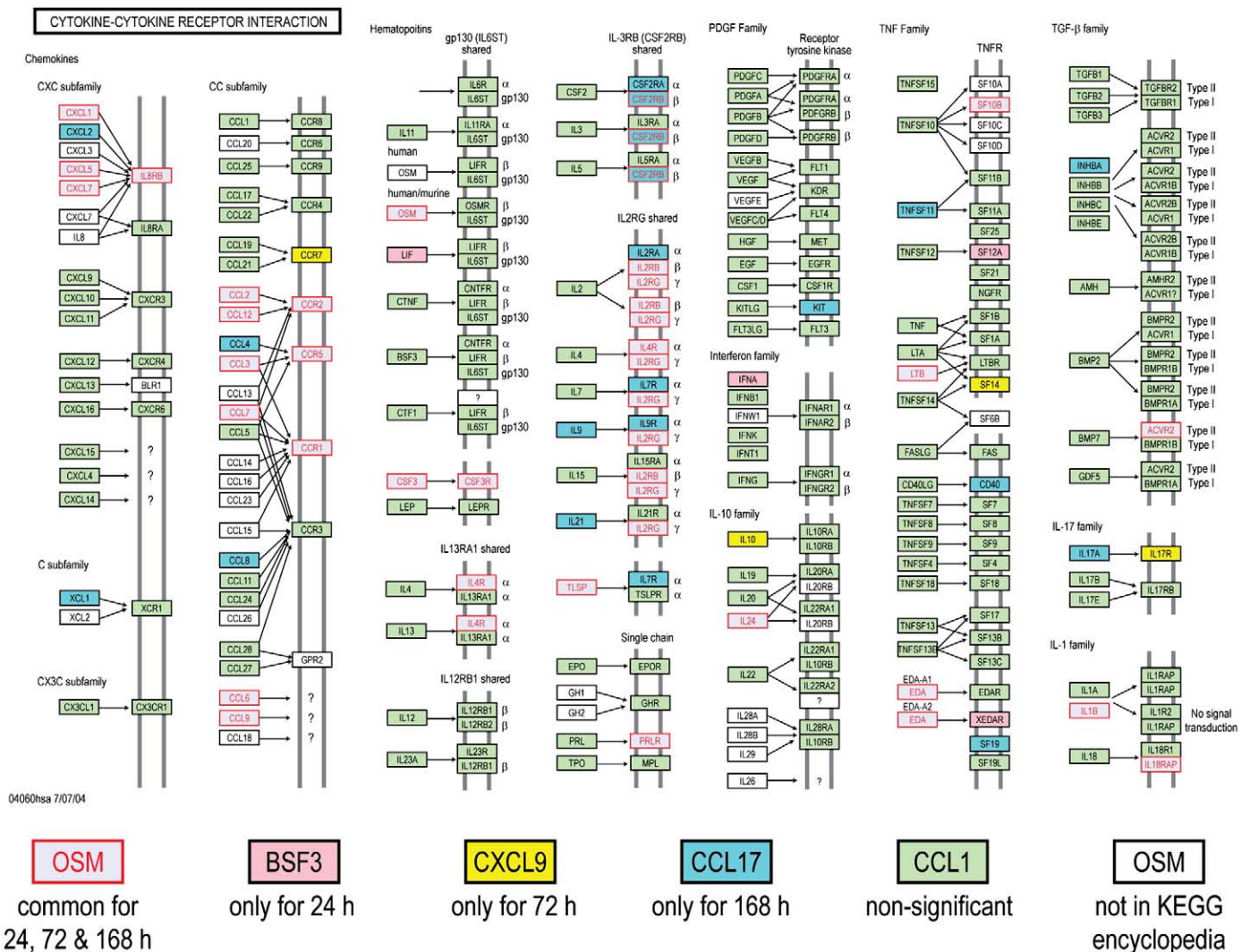


Fig. 6. Significantly expressed genes in cytokine–cytokine receptor interaction pathway disturbed by SM at different time points.

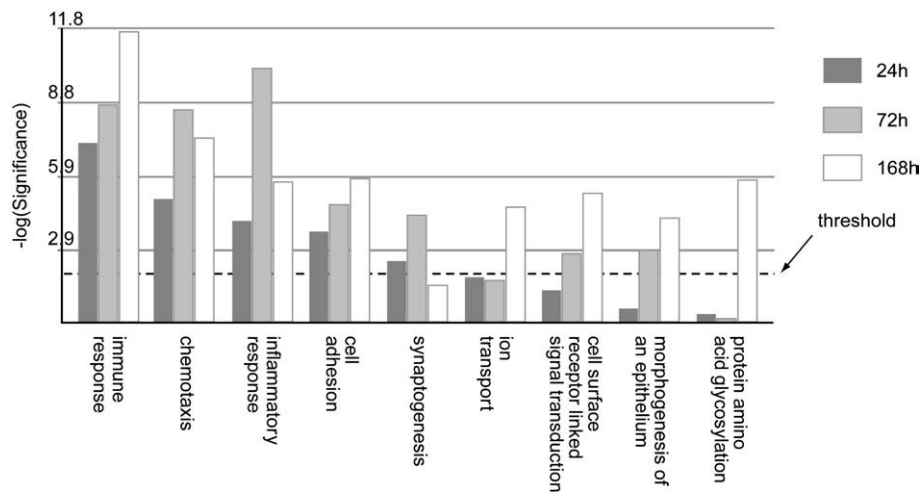


Fig. 7. Comparison of biological processes obtained by Gene Ontology analysis whose gene expression was significantly altered by SM at 24 h, 72 h and 168 h respectively. The Y-axis represents the Fisher *P* value for each biological processes shown in the X-axis. The threshold value used for screening the pathways was a *p*-value of 0.01 (i.e. $-\log_{10}(P)=2.0$).

showed that over 1000 genes were significantly expressed in mouse skin after sulfur mustard exposure. Fig. 3 depicts the hierarchical cluster analysis based on 24,681 genes with mean channel intensities in the arrays greater than 100. The control group separates from the SM-treated group, and demonstrates an increasing distance with the time after dosing. This observation indicates that an increasing number of genes are activated after SM-induced cutaneous injury. Fig. 4 shows the results from the principle component analysis based on the 24,681 genes whose mean channel intensities were greater than 100 in the arrays across different time-points after treatment. The control group clearly separated from the treated group, and a monotonous time-course trajectory of 24 h, 72 h, and 168 h was observed. This observation highlights the importance of conducting longer-term time-course studies. In the case of both the PCA and HCA analyses, a larger subject of the gene list was used (the only constraint was imposed on the channel intensity).

When a KEGG analysis was performed for different sulfur mustard post-exposure time-points, using statistically significant Fisher *P* values, novel pathway activations were identified in the sulfur mustard exposure time-points when compared to controls (Table 1). The analysis showed that cytokine–cytokine receptor interaction and the Jak-STAT signaling pathways are impacted at all the post-exposure time points. If a comparative analysis was performed in a slightly different way, using the IPA system, it would be possible to identify the top biological functions affected by sulfur mustard exposure. The data is presented in Table 2 and identifies cell death, cancer, inflammatory disease, immunological disease, and cell movement as the top biological functions affected by sulfur mustard exposure. Note that

the total number of genes affected is shown in parentheses. Table 3 shows the 46 genes involved in inflammatory response induced by sulfur mustard at different time points post-exposure. Other pathways examined include: p53 signaling (Table 4: 17 genes), NF- κ B signaling (Table 5: 25 genes), oxidative stress (Table 6: 17 genes), p38 MAPK (Table 7: 20 genes), pro-apoptosis (Table 8: 9 genes), and apoptosis (Table 9: 15 genes). Since the data carried the MEVM model out to a longer time period than previously reported, it was decided to measure the effects of MMP inhibitor I on SM-exposed skin. A list of significantly affected genes was generated utilizing the following additional constraints: cutoffs of $p < 0.05$ and fold change > 1.5). These data correspond to the green colored “common significant gene lists” in Fig. 2. A Venn diagram of the KEGG pathways meeting these criteria is presented in Fig. 5. At least 2 pathways were common for all the three time points post-exposure. One specific KEGG pathway, that of cytokine–cytokine receptor interaction pathway is presented in Fig. 6 based on a total of 240 in the ArrayTrack database. It shows the significantly expressed genes in cytokine–cytokine receptor interaction pathway which are disturbed by sulfur mustard exposure at different time points post-exposure: 51 genes at 24 h, 60 genes at 72 h, and 72 genes at 168 h, and a total of 34 common genes. Since genes that are differentially expressed can provide insight into planning further extended time studies, we performed a Gene Ontology analysis focusing on the biological processes whose gene expression was significantly altered by sulfur mustard at 24 h, 72 h, and 168 h respectively (Fig. 7). The Y-axis represents the Fisher *P* value for each biological process shown in the X-axis. There were at least four biological processes that were disturbed in all three time-points post-

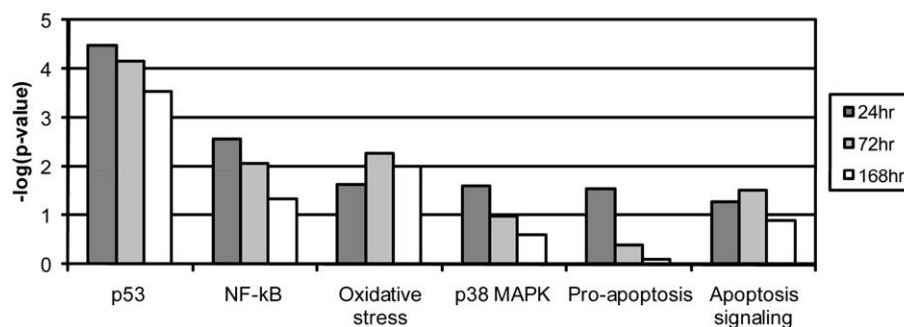


Fig. 8. Six biological pathways involved in the SM-induced cutaneous injury at 24, 72 and 168 h post-exposure. The threshold value used for screening the pathways was a *p*-value of 0.05 (i.e. $-\log_{10}(P)=1.3$).

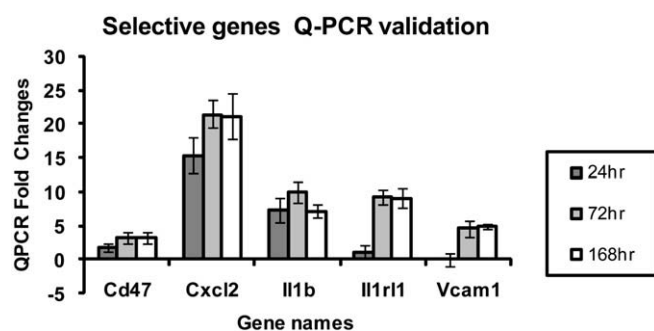


Fig. 9. Quantitation of mRNA for selected genes at various time points after treatment.

exposure. These were: immune response, chemotaxis, inflammatory response, and cell adhesion. Additional processes were disturbed with increasing post-exposure time. HCA and PCA showed no significant difference between the SM-treated and SM+inhibitor-treated cases, which was consistent with the histological information (data not shown). However, as shown in Fig. 8, the analysis of major biological pathways that were involved in sulfur mustard induced cutaneous injury showed a slightly different trend, with fewer pathways being significantly impacted with increasing time. Selected genes from the microarray data were chosen for quantitation of the mRNA. The data is presented in Fig. 9 and demonstrated that the general trends for the microarray data are consistent with the QPCR. Interleukin 1 beta was selected for protein quantitation and the data is presented in Fig. 10. The overall trends were consistent between the microarray, mRNA, and actual protein.

In order to evaluate the impact of the matrix metalloproteinase inhibitor, an alternative approach based on a predefined group of genes (through metabolic and signaling pathways obtained in KEGG) was used to evaluate differential pathway activities at each time point, post treatment, compared to the control animals. As shown in Table 10, the inhibitor treated animals show different pathway activities for 24 hour exposure. These pathways were mostly metabolic and biosynthesis related genes and represented subtle differences between the inhibitor treated and SM alone. For later responses transcriptional profiles for sulfur mustard treated and inhibitor treated samples overlap. Even though there was no significant histological difference between the SM and SM-I (i.e. with inhibitor) cases, the differential pathway activities identified here can provide insight into the time course progression of gene expression.

Discussion

One ultimate goal of vesicant research is to identify potential effective medical countermeasures to alkylation injury of the skin and to identify biomarkers for different stages of vesicant injury and wound repair. This would provide the methodology to screen large numbers of

novel compounds quickly and act as a qualitative tool to determine their potential effectiveness in alleviating damage or enhancing wound repair. One approach is to identify biomarkers that correlate to histological improvements after application of a novel countermeasure.

Microarray technology is a useful tool which provides an indication of the changing gene expression between control samples and those exposed to toxicants. In general, transcriptional analysis can generate proxies that monitor critical events associated with post-exposure changes at the cellular level; the information from transcriptional signatures can lead to development of hypotheses associated with modes of action (Androulakis, 2005). A majority of transcriptional studies to date focused on terminal events at a very coarse temporal resolution, loosely characterized as before vs. after, healthy vs. unhealthy, treated vs. vehicle, in an effort to identify clear and distinguishing variations between terminal states (Androulakis et al., 2007). However, in order to understand the progression of a phenotypic response towards a terminal state or, more importantly, the identification of “intervention” strategies, the time-evolution of the transcriptional phenomenon is critical. Additional detailed time-course experiments provide “kinetic” information on the critical points and rates associated with the post-exposure response, and can provide insight into possible interventions that alter the progression of the response. Therefore, high(er) temporal resolution transcriptional studies enable improved characterization of the cellular processes as they evolve over time thus enabling the identification of the state changes and points of intervention associated with the progress of the response. Furthermore, time-course measurements will critically assist the development of quantitative and predictive state progression models. Therefore, the present study focused on longer time periods (24, 72, and 168 h) than previously reported, in order to allow enough time for wound repair to commence.

Initial analysis used the methodology of the Gene Ontology (GO) Consortium in combination with KEGG pathway analysis. Common gene pathways for the SM-treated time-points included cytokine-cytokine receptor interaction and Jak-STAT signaling. Both of these pathways correspond to persistent inflammation, which was observed histologically as well as in the gene chip analysis (data not shown). It will be interesting to see whether the inflammatory cell population follows a defined progression from neutrophils to macrophages to mast cells over time as is true for the incisional wound model (Stramer et al., 2007). In addition to inflammatory pathways, two novel repair pathways became prominent 72 h post-treatment. These were cell communication and the Hedgehog signaling pathway, the latter of which is a pathway which plays a critical role in the regulation of the development of several tissues and organs (Ma et al., 2008). By 168 h post-treatment several additional pathways are activated including cell adhesion molecules, neuroactive ligand–receptor interactions, glycosphingolipid biosynthesis, and complement and coagulation cascades. In a broad sense, these may all be considered repair pathways. It is fully expected that additional repair pathways will turn on even later, which would require further experiments that carry the model out at least a month or more. The data

Mycroarray, QPCR and ELISA analysis data of IL-1b

Time (hr)	Treatment	Microarray-FC	QPCR-FC	Std. Error	Cytokines pg/ml
0	Naïve				< 3
24	MeCl				< 3
24	SM	35.29	7.21	1.76	4
72	MeCl				< 3
72	SM	34.18	9.98	1.55	86
168	MeCl				<3
168	SM	51.94	7.07	1	269

Fig. 10. Interleukin 1 beta microarray, QPCR, and protein data.

Table 10

An alternative approach based on a predefined group of genes (metabolic and signaling pathways in KEGG) was used to evaluate differential pathway activities at each time point, post treatment, compared to the control animals

Pathway	SM24*	SMI-24†	SM72*	SMI-72†	SM168*	SMI-168†
Neurodegenerative disorders	0.039	0.5694	0.9517	0.7433	0.7808	0.8799
Thiamine metabolism	0.04	0.1504	0.008	0.1052	0.2437	0.1894
Glioma	0.042	0.6121	0.9976	0.9944	0.9824	0.9977
Cytokine-cytokine receptor interaction	0.0456	0.0687	0.5258	0.0022	0.4987	0.0035
Terpenoid biosynthesis	0.047	0.0701	0.0011	0.0103	0.019	0.0008
Methane metabolism	0.0489	0.1945	0.0238	0.0809	0.4053	0.0456
Fatty acid biosynthesis	0.088	0.0296	0.02	0.001	0.0107	0.0041
Purine metabolism	0.1679	0.0299	0.7888	0.9612	0.6399	0.8637
Urea cycle and metabolism of amino groups	0.1408	0.031	0.9106	0.8238	0.3617	0.1675
Arachidonic acid metabolism	0.3127	0.0339	0.5819	0.0206	0.0565	0.2192
Aminosugars metabolism	0.2458	0.0393	0.2348	0.3673	0.1453	0.3668
Cell communication	0.337	0.0427	0.376	0.0164	0.0564	0.075
Taurine and hypotaurine metabolism	0.2754	0.0429	0.9024	0.6113	0.5074	0.2642
Glycosylphosphatidylinositol	0.4842	0.048	0.7613	0.5648	0.8792	0.2443
Nicotinate and nicotinamide metabolism	0.2134	0.1421	0.0032	0.1505	0.1291	0.3936
Bile acid biosynthesis	0.6092	0.1469	0.0032	0.0214	0.0486	0.0336
Riboflavin metabolism	0.1653	0.1599	0.004	0.1066	0.0129	0.2346
1- and 2-Methylnaphthalene degradation	0.1686	0.1244	0.0046	0.0497	0.0196	0.0486
Fatty acid elongation in mitochondria	0.3335	0.5421	0.0083	0.1426	0.5593	0.2223
Metabolism of xenobiotics by cytochrome P450	0.6824	0.2559	0.0116	0.06	0.4679	0.1099
Lysine degradation	0.4443	0.487	0.0132	0.0467	0.2505	0.117
Fatty acid metabolism	0.3226	0.2493	0.014	0.0486	0.1827	0.1152
gamma-Hexachlorocyclohexane degradation	0.3418	0.158	0.018	0.049	0.0495	0.055
Sulfur metabolism	0.6127	0.5662	0.0223	0.671	0.3992	0.2367
Tryptophan metabolism	0.7325	0.2778	0.0266	0.07	0.603	0.1552
Styrene degradation	0.2302	0.06	0.0278	0.0916	0.264	0.0721
Carbazole degradation	0.8657	0.7966	0.0281	0.18	0.0181	0.0244
Androgen and estrogen metabolism	0.8155	0.3289	0.0293	0.1141	0.6005	0.1842
Reductive carboxylate cycle	0.3027	0.3365	0.0367	0.0886	0.189	0.2233
Glutathione metabolism	0.355	0.3515	0.0405	0.1432	0.2103	0.2079
1,1,1-Trichloro-2,2-bis	0.9007	0.8062	0.0435	0.2153	0.0213	0.0342
Valine, leucine and isoleucine degradation	0.7407	0.231	0.0438	0.0322	0.1719	0.0539
2,4-Dichlorobenzoate degradation	0.8281	0.3744	0.0462	0.1379	0.0491	0.0327
Benzoate degradation via CoA ligation	0.298	0.2447	0.047	0.0403	0.1013	0.0856
Hematopoietic cell lineage	0.5299	0.071	0.0476	0.8882	0.7409	0.1487
Synthesis and degradation of ketone bodies	0.6306	0.2081	0.0954	0.0163	0.0537	0.0238
Pantothenate and CoA biosynthesis	0.3431	0.1294	0.1956	0.0213	0.0097	0.0085
Propanoate metabolism	0.1823	0.1216	0.0747	0.0287	0.0852	0.0507
Butanoate metabolism	0.8944	0.2828	0.1042	0.0294	0.1885	0.0544
Biosynthesis of steroids	0.189	0.1281	0.0525	0.0295	0.0856	0.0238
Linoleic acid metabolism	0.1662	0.351	0.2802	0.033	0.1353	0.098
Lysine biosynthesis	0.4334	0.0943	0.4849	0.0332	0.2065	0.0709
Glycine, serine and threonine metabolism	0.639	0.3086	0.1198	0.0363	0.1768	0.0851
Pyruvate metabolism	0.5949	0.7417	0.1988	0.0371	0.1988	0.067
ABC transporters - general	0.2504	0.2368	0.3741	0.4469	0.0185	0.2165
Circadian rhythm	0.1174	0.0515	0.3505	0.2296	0.0414	0.0762
Inositol metabolism	0.0754	0.0517	0.1752	0.7487	0.3397	0.029
Vitamin B6 metabolism	0.4674	0.2128	0.5157	0.0751	0.08	0.0325

Inhibitor treated animals show different pathway activities for 24 h exposure. For later responses transcriptional profiles for sulfur mustard treated and inhibitor treated samples overlap. Even though there was no significant histological difference between the SM and SM-I (i.e. with inhibitor) cases, the differential pathway activities identified here can provide insight into the time course progression of gene expression. The table depicts the *p*-values associated with the confidence level that there was significant change in the activity of a particular pathway under a specific condition. Gray shaded entries correspond to *p*-values less than 0.05 and hence express confidence that a particular pathway was indeed altered at that condition.

* Exposure to sulfur mustard only.

† Exposure to Sulfur Mustard plus Inhibitor.

were analyzed a slightly different way, sorting according to the top biological functions, and similar results occurred. The biological functions included inflammation, immunological activation, cell movement, and cell death, also supporting the notion that cells are actively dividing and migrating in an attempt to heal the wound. These data are consistent with the belief that inflammation is persistent and a long-term process in the MEVM. In fact, genes involved in the inflammatory pathway topped the list in every type of analysis performed in this study. The most significant individual mRNA increase was for CXCL2 (also called MIP-2, macrophage inflammatory protein-2) and increased by a tremendous 500 fold by 168 h post-treatment (Table 3). This protein is involved with neutrophil recruitment and other inflammatory processes, so CXCL2 upregulation was not unexpected. Other inflammatory genes significantly upregulated after sulfur mustard exposure included CCL2, CCR1, Il1b, Il6, and PTGS2. All of these increased dramatically by

24 h post-SM exposure, demonstrating the value of analyzing early time points as well as the later ones. Several of these cytokines and Vcam1 were chosen for quantitation of their mRNA for the various time points (Fig. 9). In every case the mRNA validated the general trends of the microarray data. In order to validate that mRNA is translated into protein, interleukin 1 beta was quantitated and agreed with the microarray and mRNA data (Fig. 10). The major gene pathways affected by sulfur mustard were predominantly inflammatory, apoptosis, and stress-related pathways (Tables 3–9). These all reflect the severity of the wound caused by sulfur mustard exposure. Testing an inhibitor of matrix metalloproteinase activity demonstrated that subtle, but specific changes do occur in the gene profiles when microarray analysis is performed (Table 10). Since these changes are more quantitative than the histological changes which are more qualitative (evaluating amount of edema, number of invading inflammatory cells, and severity of

necrosis), these differences in microarray patterns may correlate to predictable changes in SM exposed skin and lead to the identification of biomarkers for specific stages of injury. The pathway changes observed in the inhibitor I microarrays involved the metabolism, degradation, and biosynthesis of many molecules suggesting that the wound healing response was slightly accelerated using MMP-2/9 inhibitor I, although no gross changes in inflammation, or inflammatory genes were noted.

Taken together, the microarray data provide detailed information regarding the genes that become activated in mouse skin following exposure to sulfur mustard. Many of these genes reflect biologic processes. In general, a host of cytokines and mediators of inflammation are released and activated early (within 24 h) after SM exposure. These include genes in the NF κ B pathway and the p38 MAP kinase pathway. Hyperproliferation and cell division are also activated early as seen by a number of genes under control of the p53 signaling pathway. Apoptosis and oxidative stress genes also turn on early and remain on throughout all the time points observed. When this methodology was applied to the MMP-2/MMP-9 inhibitor I data, there were numerous repair process genes that became activated when compared to SM-alone treated samples. This demonstrates the sensitivity of the assay since we did not observe any quantitative histological differences between SM-alone and MMP inhibitor I treated samples. If these results can be replicated and the same genes that were activated in this system identified, there is potential for use of microarrays as markers of repair.

Although the data were analyzed in several different ways, the major results were similar, depending on the analysis employed. However, there were subtle differences between the various analyses. Regardless of the different results, all the methods were valid and useful in analyzing gene expression at different time periods post-exposure. Higher time resolution gene expression experiments, partly performed in this study, beyond the standard dose–response analysis, will significantly boost the ability to cross over from the present, mostly, descriptive nature of genomics towards a more useful mathematical model-based analysis that identifies specific phases of wound progression and repair in order to develop targeted medical interventions. Microarray analysis shows strong potential for advancing the knowledge of the MEVM system and for use as a prescreening tool to predict the general effectiveness of medical countermeasures to vesicant injury.

Acknowledgments

This research was supported in part by the following grants: NIEHS sponsored UMDNJ Center for Environmental Exposures and Disease (Grant # NIEHS P30ES005022); NIH/NIEHS funded Training

in Environmental Toxicology (ES004738); NIH/NEI funded Expression of Specialized Collagens in Cornea (EY09056); NIH funded CounterACT Program (NIAMS U54AR055073); and USEPA STAR Grant funded Environmental Bioinformatics and Computational Toxicology Center (GAD R 832721-010). Its contents are solely the responsibility of the authors and do not necessarily represent the official views of the funding agencies including NIH, USFDA, and USEPA. Appreciation is extended to Linda Everett of EOHSI for editorial assistance.

References

- Androulakis, I.P., 2005. Selecting maximally informative genes. *Comput. Chem. Eng.* 29, 535–546.
- Androulakis, I.P., Yang, E., Almon, R.R., 2007. Analysis of time-series gene expression data: methods, challenges, and opportunities. *Annu. Rev. Biomed. Eng.* 9, 205–228.
- Cowan, K.N., Jones, P.L., Rabinovitch, M., 2000. Elastase and matrix metalloproteinase inhibitors induce regression, and tenascin-C antisense prevents progression, of vascular disease. *J. Clin. Invest.* 105, 21–34.
- Dillman III, J.F., Hege, A.L., Phillips, C.S., Orzolek, L.D., Sylvester, A.J., Bossone, C., Henemyre-Harris, C., Kiser, R.C., Choi, Y.W., Schlager, J.J., Sabourin, C.L., 2006. Microarray analysis of mouse ear tissue exposed to bis-(2-chloroethyl) sulfide: gene expression profiles correlate with treatment efficacy and an established clinical endpoint. *J. Pharmacol. Exp. Ther.* 317, 76–87.
- Ingenuity Systems, 2008. Ingenuity Pathways Analysis (IPA).
- Kanehisa, M., Goto, S., Kawashima, S., Okuno, Y., Hattori, M., 2004. The KEGG resource for deciphering the genome. *Nucleic Acids Res.* 32, D277–D280.
- Ma, G., Xiao, Y., He, L., 2008. Recent progress in the study of Hedgehog signaling. *J. Genet. Genomics* 35, 129–137.
- Monteiro-Riviere, N.A., Inman, A.O., Babin, M.C., Casillas, R.P., 1999. Immunohistochemical characterization of the basement membrane epitopes in bis(2-chloroethyl) sulfide-induced toxicity in mouse ear skin. *J. Appl. Toxicol.* 19, 313–328.
- Powers, J.C., Kam, C.M., Ricketts, K.M., Casillas, R.P., 2000. Cutaneous protease activity in the mouse ear vesicant model. *J. Appl. Toxicol.* 20 (Suppl. 1), S177–S182.
- Rogers, J.V., Choi, Y.W., Kiser, R.C., Babin, M.C., Casillas, R.P., Schlager, J.J., Sabourin, C.L., 2004. Microarray analysis of gene expression in murine skin exposed to sulfur mustard. *J. Biochem. Mol. Toxicol.* 18, 289–299.
- Sabourin, C.L., Rogers, J.V., Choi, Y.W., Kiser, R.C., Casillas, R.P., Babin, M.C., Schlager, J.J., 2004. Time- and dose-dependent analysis of gene expression using microarrays in sulfur mustard-exposed mice. *J. Biochem. Mol. Toxicol.* 18, 300–312.
- Shakarjian, M.P., Bhatt, P., Gordon, M.K., Chang, Y.C., Casbohm, S.L., Rudge, T.L., Kiser, R.C., Sabourin, C.L., Casillas, R.P., Ohman-Strickland, P., Riley, D.J., Gerecke, D.R., 2006. Preferential expression of matrix metalloproteinase-9 in mouse skin after sulfur mustard exposure. *J. Appl. Toxicol.* 26, 239–246.
- Stramer, B.M., Mori, R., Martin, P., 2007. The inflammation-fibrosis link? A Jekyll and Hyde role for blood cells during wound repair. *J. Invest. Dermatol.* 127, 1009–1017.
- Tong, W., Cao, X., Harris, S., Sun, H., Fang, H., Fuscoe, J., Harris, A., Hong, H., Xie, Q., Perkins, R., Shi, L., Casciano, D., 2003. ArrayTrack-supporting toxicogenomic research at the U.S. Food and Drug Administration National Center for Toxicological Research. *Environ. Health Perspect.* 111, 1819–1826.
- Tong, W., Harris, S., Cao, X., Fang, H., Shi, L., Sun, H., Fuscoe, J., Harris, A., Hong, H., Xie, Q., Perkins, R., Casciano, D., 2004. Development of public toxicogenomics software for microarray data management and analysis. *Mutat. Res.* 549, 241–253.
- Yancey, K.B., 2005. The pathophysiology of autoimmune blistering diseases. *J. Clin. Invest.* 115, 825–828.